UNRAVELING UNEXPECTED SNOWMELT CHANNELS: A CASE STUDY IN THE AUSTRIAN ALPS

Veronika Hatvan[1]*, Andreas Gobiet[1], Andreas Riegler[1], Ingrid Reiweger[2]

[1] *GeoSphere Austria, Vienna, Austria*
[2] *BOKU University of Natural Resources and Life Sciences, Department of Civil Engineering and Natural Hazards, Institute of Mountain Risk Engineering, Vienna, Austria*

ABSTRACT: Snowmelt channels on the snow surface are frequently observed and reported phenomena, typically associated with rain-on-snow events. Consequently, they often serve as indicators of the approximate elevation of the snow line—a critical factor in assessing wet-snow avalanche conditions and snow cover stability in general. Direct field observations and feedback obtained from field assessments constitute an invaluable component for operational avalanche forecasting, offering critical insights into snowpack conditions and associated avalanche hazards. Accurate interpretation of these observations, along with a detailed understanding of underlying processes, is imperative for developing a comprehensive overall understanding of snow cover conditions as a basis for precise avalanche warnings. Recent observations of the development of snowmelt channels without notable liquid precipitation challenged the assumption of rain-on-snow events being the sole formation process. We consequently performed a study aiming to comparatively quantify liquid water input into the snow cover from melt processes as well as rain in conditions when snowmelt channels form. Through a combination of observations, energy balance calculations and model simulations, our objective is to gain a deeper understanding of the processes involved to potentially challenge the common hypothesis, that snowmelt channels are a reliable indicator of preceding rain-on-snow.

KEYWORDS: snowmelt channels, rain-on-snow, snowmelt, wet-snow

1. INTRODUCTION

Visual observations of snow cover features are essential in avalanche forecasting. They provide real-time data on snowpack conditions, enhancing avalanche risk assessments. Importantly, such data can also be communicated to avalanche warning services by individuals with varying levels of expertise, including non-experts or less trained personnel, thereby enriching the overall information available. However, accurate interpretation of such observations requires a profound understanding of the underlying processes that lead to the observed surface features, ensuring the correct integration of this information into avalanche forecasting.

Rain or meltwater channels, also known as rills, are among the surface features frequently reported from the field. These features arise from liquid water percolating through the snow, concentrating into sub-surface flow channels, with the degree of impact varying according to the amount of liquid water and the original characteristics of the dry snow. The locally accelerated settlement of the snowpack is manifested as surface rills that trace the path of these subsurface flow channels (LaChapelle, 2001) The international classification for seasonal snow on the ground (Fierz et al., 2009) describes these elements of surface roughness as “convex furrows” or “melt groves” attributed to rain or melt processes.

However, among many avalanche forecasters the formation of these surface channels or rills is commonly attributed solely to rain-on-snow (ROS) events. Based on this, these channels are frequently used as indicators for determining the elevation of the snow line - the transition from snowfall to rain - during precipitation events. Additionally, they serve as indicators for wet-snow avalanche conditions and the overall condition of the snowpack.

Recent observations of such channels have challenged the widely accepted attribution of their formation solely to rain-on-snow (ROS) events, with reports of extensive channel development occurring in the absence of significant liquid precipitation. This suggests that melt processes, as suggested in the literature (e.g. Fierz et al., 2009; International Association of Hydrological Sciences, 1981) also play an important role in the formation of these channels, a factor that is often unjustly overlooked.

This study aims to compare the liquid water input from melt processes with that from liquid precipitation during the formation of widespread snowmelt channels in December 2023 in Styria, Austria. By combining field observations, measurements, as well as model simulations, our study

* *Corresponding author address:*
Veronika Hatvan, GeoSphere Austria, Salzburg, Austria;
tel: +43 664 8849 3515;
email: veronika.hatvan@geosphere.at

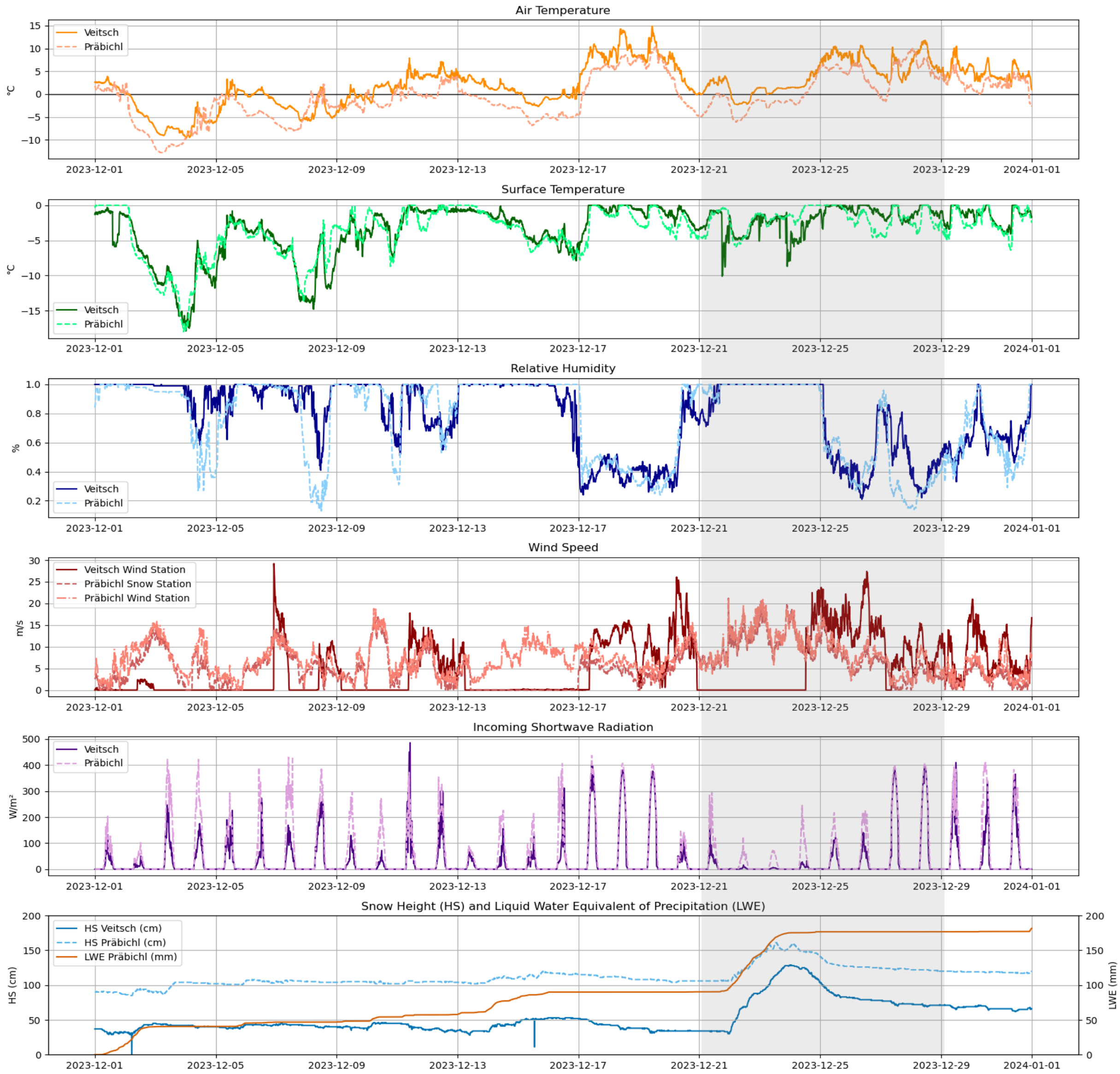

Figure 1: Meteorological observations from Automatic Weather Stations (AWS) at two sites: Veitsch and Präbichl. At Veitsch, data were collected at a snow station located at 1323 m ASL and a wind station at 1973 m ASL. At Präbichl, measurements included precipitation at 1214 m ASL, snow height at 1690 m ASL, and combined snow and wind observations at 1731 m ASL, with an additional wind station at 1907 m ASL. The dataset covers the period from December 1, 2023, to December 31, 2023. The shaded region indicates the specific period analysed in the case study. The lowermost panel provides a comparison between measured precipitation (expressed as liquid water resp. liquid water equivalent) and snow height measurements at the two snow stations.

seeks to deepen the understanding of the processes contributing to snowmelt channel development.

2. SNOW AND WEATHER OBSERVATIONS IN DECEMBER 2023

Following initial snowfall events at alpine elevations (>2000 m ASL) in early November, a continuous snow cover formed at mid-elevations (around 1500 m ASL) from mid-November onward. Variable weather conditions, characterised by repeated precipitation and occasional rain-on-snow (ROS) events at alpine elevations, followed by cold periods with snowfall and wind, resulted in a rather heterogeneous early-winter snowpack structure.

From mid-December, the onset of a pronounced Azores High brought several days of mild and sunny weather to the Eastern Alps, with temperatures reaching up to +8°C at 2000 meters ASL (see Fig. 1 uppermost panel – air temperatures at 1323 m ASL at automatic weather station (AWS) Veitsch reach 15°C on 18. & 19.12.2023). This warm period caused the snowpack to settle and by 21.12.2023 a compact snow base had developed, primarily composed of multiple melt-freeze crusts interspersed with various stages of partly moist decomposed or fragmented particles.Beginning on 22.12.2023, a shift to a stormy northwest weather pattern led to significant snowfall, particularly along the northern flanks the Alps where orographic precipitation frequently contributes to large precipitation amounts. Automatic weather stations in our study region measured snowfall accumulations of 60 to 100 cm within approximately 48 hours (22 - 24.12.2023, see Fig. 1 lowermost panel) during this snowfall event. Despite a decrease in air temperatures compared to the preceding warm period, snowfall occurred at relatively high temperatures, around or slightly above 0°C, resulting in a warm layer of fresh snow (see Fig. 1, uppermost panel).

The snowstorm ended on 24.12.2023, followed by an abrupt return of warm air masses into the Eastern Alps. Due to the warm conditions, the snowpack stabilised rapidly, becoming compact and free of significant weak layers, even at higher elevations.

Figure 2: Webcam imagery from the Brunnalm – Hohe Veitsch ski area, capturing a view of terrain with elevations ranging approximately from 1600 to 1700 m ASL. The upper panel shows a webcam image from December 24, 2024, at 09:00 UTC, depicting an undisturbed, evenly distributed fresh snow surface following a snowfall event that ended during the previous night. The lower panel presents a webcam image from December 25, 2024, at 08:00 UTC, showing the formation of well-pronounced meltwater channels on the snow surface.

In summary, by the end of December, conditions resembled those typically seen in spring, even at high altitudes

Observations of meltwater channels on the snow surface were documented immediately following the precipitation event. In the morning of 25.12.2023, avalanche forecasters from the Styrian Avalanche Warning Service reported the presence of widespread meltwater channels during a field investigation at Präbichl area, extending up to an elevation of at least 1900 m ASL. Similar observations were concurrently captured via webcams in the region, including in the Veitsch/Brunnalm ski area (see Fig. 2). Initially, an intense rain-on-snow (ROS) event during the night of 24.12 to 25.12.2023 was suspected as the cause. However, subsequent data analysis indicated only minimal sleet or rainfall/drizzle during that period, raising questions about the factors contributing to the pronounced and widespread development of the observed meltwater channels.

3. POTENTIAL MELTWATER PRODUCTION VS. LIQUID PRECIPITATION

To identify the factors driving the observed meltwater channel event, we quantified the energy available for melting and subsequently assessed the potential cumulative snowmelt. This analysis was conducted using data from an automatic weather station located in proximity to the meltwater channel observation site, at Hohe Veitsch. This station, equipped with a CNR4 net radiometer (Kipp & Zonen, 2024) provided the necessary measurements to calculate a full surface energy balance EB_{surf}:

$$EB_{\mathrm{surf}} = Q_{\mathrm{LW}} + Q_{\mathrm{SW}} + H + E \quad \left[\frac{W}{m^2}\right] \qquad (1)$$

Where Q_{LW} and Q_{SW} are net long- and shortwave radiation calculated directly from the CNR4 measurements. H is the sensible heat flux calculated by

$$H = C_{\mathrm{Bulk}} \times \rho_{\mathrm{air}} \times cp_{\mathrm{moist}} \times VW \times (T_{\mathrm{air}} - T_{\mathrm{surf}}) \qquad (2)$$

with C_{Bulk}being the dimensionless bulk heat transfer coefficient. For the purposes of the calculations presented in this study, a conservative dimensionless bulk transfer coefficient, $C_{\mathrm{Bulk}} = 0.002$ was adopted for both heat and water vapour transfer, as suggested from literature for a flat snow surface under statically neutral conditions (Kondo and Yamazawa, 1986).

ρ_{air} is calculated by the ideal gas law, using the calculated water vapour pressure e (see Eq.5) and the air pressure at AWS Veitsch, calculated by the barometric equation based on air pressure and air temperature measurements from AWS Präbichl and AWS Veitsch. The heat capacity of moist air $cp_{\mathrm{moist}} = cp_{\mathrm{air}} + q_{\mathrm{air}} \times cp_{\mathrm{vapour}}$ has been calculated using the specific humidity q_{air} (see Eq.4). $VW\ [\frac{m}{s}]$, T_{air} and $T_{\mathrm{surf}}\ [K]$ are measured wind speed, air temperature and snow surface temperature, respectively.

The latent heat flux E is calculated by

$$E = L_{\mathrm{v}} \times \rho_{air} \times C_{\mathrm{BULK}} \times VW \times (q_{\mathrm{air}} - q_{\mathrm{surf}}), \qquad (3)$$

where $L_{\mathrm{v}} = 2.5 \times 10^6\ [\frac{J}{kg}]$ is the latent heat of vaporization, q_{air} and q_{surf} are the specific humidity of air and the snow surface respectively, calculated by

$$q = \frac{0.622 \times e}{p - e}, \qquad (4)$$

using the calculated air pressure p at AWS Veitsch and the water vapour pressure e

$$e = RH \times e_{sat} \qquad (5)$$

calculated from the saturation vapour pressure e_{sat}, the measured relative humidity (RH) and temperature:

$$e_{\mathrm{sat}} = 6.112 \times exp^{\frac{17.67 \times (T - 273.15)}{T - 29.65}}. \qquad (6)$$

For the snow surface we assume saturation, meaning that RH = 1 (100%) and $e = e_{\mathrm{sat}}$, with e_{sat} calculated using the measured snow surface temperature T_{surf}. The ground heat flux is assumed to be negligible for this surface energy balance approach.

From the surface energy balance we subtracted the energy needed to heat the upper 1 cm of snow to the melting point (0°C) using the formula

$$Q_{\mathrm{heat}} = cp_{\mathrm{snow}} \times v_{\mathrm{snow}} \times \rho_{\mathrm{snow}} \times (273.15 - T_{\mathrm{surf}}) \qquad (7)$$

With $cp_{\mathrm{snow}} = 2100\ \frac{J}{kgK}$ being the heat capacity of ice resp. snow, $v_{\mathrm{snow}} = 0.01\ m^3$ the volume of snow and $\rho_{\mathrm{snow}} = 150\ \frac{kg}{m3}$ the assumed density of the fresh snow layer.

The energy available for melt Q_{melt} was calculated by

$$Q_{\mathrm{melt}} = EB_{\mathrm{surf}} - Q_{\mathrm{heat}} \qquad (8)$$

and subsequently used to calculate potential meltwater production

$$M_{\mathrm{melt}} = \frac{Q_{\mathrm{melt}}}{L_{\mathrm{f}} \times \rho_{\mathrm{water}}}\ [mm\ or\ \frac{l}{m^2}]$$

with $L_{\mathrm{f}} = 3.34 \times 10^5 \left[\frac{J}{kg}\right]$ and $\rho_{\mathrm{water}} = 1000 \left[\frac{kg}{m^3}\right]$.

For this calculation, we utilised meteorological and radiation balance data from AWS Veitsch. However, due to a frozen sensor, wind measurements were unavailable from 22.12 to 24.12.2023. To address this data gap, we supplemented the analysis with wind data from AWS Präbichl, which was used for additional energy balance and meltwater calculations.

As illustrated in Figure 1 (4th panel from the top), wind speeds were measured at two locations at AWS Präbichl. Both measurements are continuous and

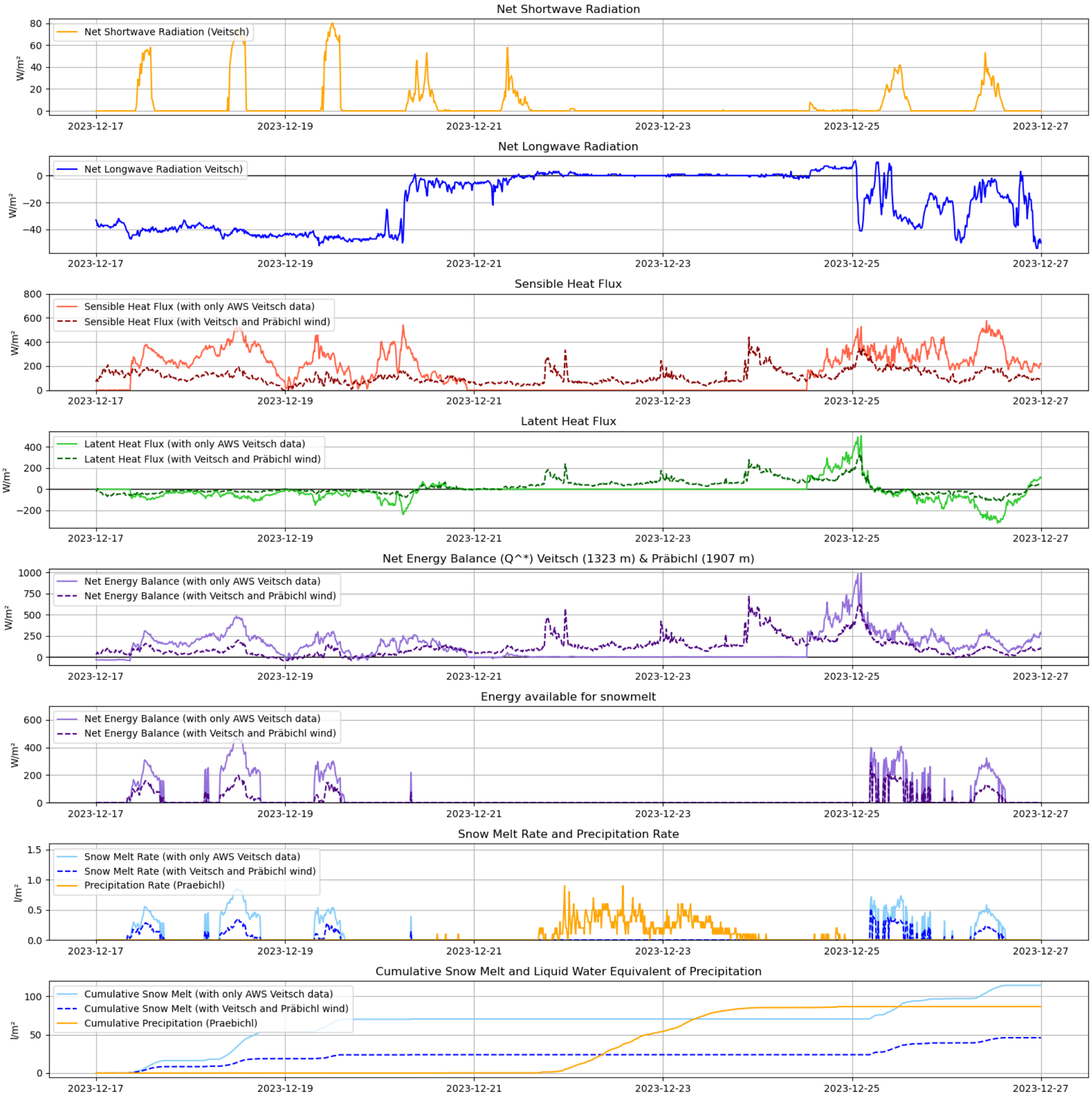

Figure 3: Energy balance terms calculated based on measurements from AWS Veitsch, with partial incorporation of wind data from AWS Präbichl. The figure also presents cumulative values of potential meltwater production and the liquid water equivalent of precipitation, alongside the calculated meltwater production rates derived from the energy balance calculations and the measured precipitation rates at AWS Präbichl.

consistently recorded lower wind speeds compared to AWS Veitsch. Although the two sites at AWS Präbichl differ by a few hundred meters in elevation, their wind speed readings were similar, with slightly lower values at the snow station.

Given that wind stations are typically in exposed locations, which may not fully represent conditions at the snow height and radiation balance measurement sites at AWS Veitsch, the wind measurement from the Präbichl snow station was deemed more suitable for representative energy balance calculations.

Figure 3 illustrates the calculated surface energy balance terms along with the cumulative values of the potential meltwater production and the liquid water equivalent of precipitation during the period from 17.12 2023 to 27.12 2023. The precipitation measurements at AWS Präbichl (shown in the lowermost and second-lowest panels) clearly reflect the observed weather pattern, indicating approximately 100 mm of liquid water equivalent of precipitation between 22.12.2023 and 24.12.2023.

At the elevation of the snow stations, most of this precipitation fell as fresh snow, as depicted in the lowest panel of Figure 1. The main phase of precipitation ended around midnight on 23.12.2023.

Subsequently, only 1.3 mm of liquid water equivalent of precipitation was measured at AWS Präbichl between 12 UTC on 24.12.2023, 12 UTC and

25.12.2023, 12 UTC, during which time meltwater channels were observed. During this period, air temperatures at the AWS location had already risen above 0°C, suggesting that any precipitation that fell did so in liquid form. However, at higher elevations, different conditions may have prevailed. During the same period, approximately 7 mm and 10 mm of potential meltwater production were calculated based on the use of AWS Präbichl wind data and exclusively on AWS Veitsch measurements, respectively.

Even larger amounts of potential meltwater production were calculated for the period prior to Christmas, between 17.12 and 20.12.2023. During this time, high temperatures and sunny, cloudless conditions resulted in a positive energy balance. However, no meltwater channels were observed during this period. This absence of channels might be attributed to the low relative humidity, which likely led to increased evaporation. Additionally, the significantly different snow cover conditions, characterised by a hard and compact snow surface with a well-settled base, likely slowed the percolation of liquid water, preventing the formation of meltwater channels.

4. MODELLING RESULTS

Based on data from AWS Präbichl, we conducted snow cover simulations using the SNOWPACK model. For the purpose of this study, we focus on the liquid water content and snow temperature, which indicate that liquid water began penetrating the snow cover during the night and morning of 25.12.2023 (see Fig. 4). The onset of snowpack wetting appears to coincide with the liquid precipitation observed in the afternoon and evening of 24.12.2023. However, full liquid water penetration of the snowpack only progressed beyond the uppermost layers during the night, even in the absence of further liquid precipitation. This suggests that the model also detects meltwater production during this period.

In contrast, during an earlier warm period between 17.12 and 20.12.2023, liquid water did not penetrate the snowpack beyond the uppermost centimetres. Despite the high air temperatures observed during this earlier period (see Fig. 1, uppermost panel), the depth of liquid water penetration was reduced compared to the conditions on 25.12.2023. This difference suggests that a greater portion of the available energy was used for evaporation, driven by the very dry and cloudless atmosphere at that time (see Fig. 1, relative humidity and Fig. 3, net longwave radiation). This comparison underscores the significant influence of atmospheric conditions on the energy distribution between melting and evaporation, affecting the depth of snowpack wetting and the overall meltwater production and liquid water penetration. The modelled snow temperatures suggest that the fresh snow had very little cold reserve, meaning that the snowpack quickly responded to the energy input, leading to rapid warming and subsequent wetting.

5. DISCUSSION

The calculated potential meltwater produced during the morning of 25.12.2023, is considerably larger than the accumulated liquid water from rain during

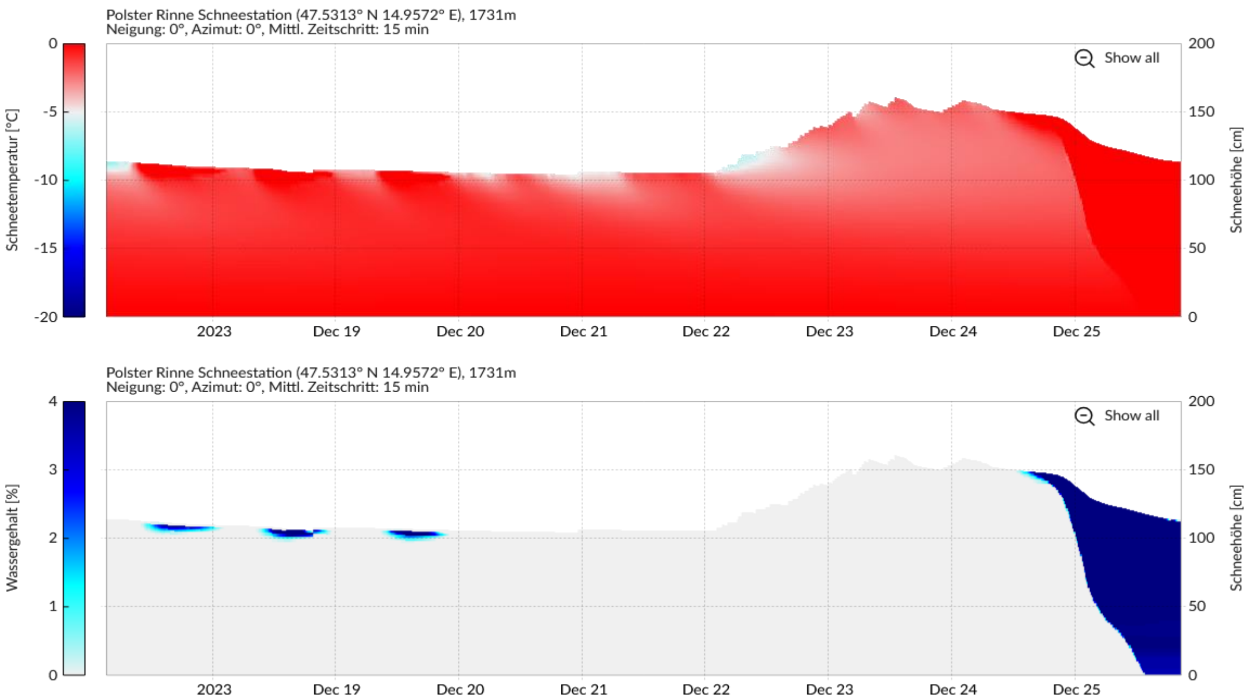

Figure 4: SNOWPACK model results for the period between 17.12. and 25.12.2023, based on measurements from AWS Präbichl. The top panel shows snow temperatures, while the bottom panel displays the liquid water content within the snowpack.

the evening of 24.12.2023. Although larger, both quantities remain within the same order of magnitude. This indicates that both processes likely contributed comparably to the formation of the meltwater channels, with atmospheric conditions potentially determining which process becomes more dominant.

Given these numbers, it becomes even more critical to acknowledge that the estimated amount of meltwater production should be regarded as an approximation. This estimate is influenced by several assumptions made during the calculation process, which inevitably affect its accuracy.

In addition to the inherent measurement errors associated with all data collection, this study specifically addressed a systematic bias in snow surface temperature measurements. These errors typically become apparent during snowmelt periods when the snow surface temperature of a continuous snow cover should be constrained to a maximum value 0°C. For the calculations presented above, the surface temperature T_{surf} recorded at the AWS Veitsch was adjusted for a positive systematic bias of 1°C. This adjustment involved systematically reducing the recorded temperatures across the entire season and, even after making these adjustments, capping all values at 0°C whenever snow was present. The accuracy of this systematic bias correction is critical for the calculation of Q_{heat}– the amount of energy required to raise the snow surface temperature to 0°C – which significantly impacts the amount of available energy for the melting process. This calculation is further dependent on the assumption that only the uppermost centimetre of the snow cover is raised to 0°C. The impact of this correction becomes even more pronounced with a larger volume of snow being raised to 0°C, thereby intensifying its effect on the overall energy balance.

Another issue concerning data quality and availability involves the calculation of turbulent fluxes, which relied on wind speed measurements from exposed wind stations. These measurements may not accurately reflect wind speeds further down the slope or at the location of the meteorological sensors, likely leading to an overestimation of the turbulent heat fluxes.

The surface energy balance calculation is also heavily dependent on the choice of the bulk transfer coefficient C_{Bulk}, which depends on atmospheric stability and surface roughness. In this analysis, a conservative approach was taken by selecting a relatively low bulk transfer coefficient appropriate for statically neutral atmospheric conditions over flat snow covered terrain. However, in structured terrain and under unstable atmospheric conditions, the bulk transfer coefficient can be significantly larger (Wallace and Hobbs, 2006) and would result in significantly larger turbulent fluxes, thereby impacting the energy balance of the snow surface.

For simplicity, we assumed that the entire available energy would be used solely for snowmelt. However, the partitioning of energy between snowmelt and evaporation is highly dependent on atmospheric conditions. During very dry atmospheric conditions, such as those characterised by low relative humidity, a greater proportion of the energy would be allocated to snow evaporation. This phenomenon is particularly evident e.g. during Föhn storm situations in the Alps, where warm and dry air is advected over the snow surface. In such cases, a significant portion of the energy is used for snow evaporation, resulting in a notably dry snowpack, less snowmelt and no meltwater channels.

Additionally, the characteristics of the snowpack likely played a significant role in the melting process. The warm air temperatures during the snowfall contributed to the formation of a fresh snow layer with very limited cold reserves. Consequently, only a small amount of energy was required to raise the temperature of the snowpack to 0°C. Once this minimal energy input was met, any additional energy available was directed toward melting, as observed in this case study. This condition accelerates the onset of snowmelt and can lead to faster and more extensive melting compared to a snowpack with larger cold reserves.

6. CONCLUSION

The study challenges the widely held assumption that meltwater channels are formed exclusively by rain-on-snow events, revealing that meltwater generated from a positive energy balance can also contribute to their development. By analysing snowpack characteristics, meteorological data, energy balance calculations and model simulations, the study demonstrated that atmospheric and snowpack conditions play a crucial role in meltwater channel formation. Despite the conservative approach taken in the analysis, the findings clearly indicate that liquid water generated from a positive energy balance, rather than solely from liquid precipitation, also plays a role in the development of these channels. While this case study does not provide a definitive conclusion, it strongly suggests the need for further investigation into the processes governing meltwater channel production.

REFERENCES

Fierz, C., Armstrong, R. L., Durand, Y., Etchevers, P., Greene, E., McClung, D. M., Nishimura, K., Satyawali, P. K., and Sokratov, S. A.: The international classification for seasonal snow on the ground. Prepared by the ICSI-UCCS-IACS working group on snow classification, 2009.

International Association of Hydrological Sciences, . International Commission on Snow and Ice: Avalanche atlas: illustrated international avalanche classification, UNESCO, Paris, 265 pp., 1981.

Kondo, J. and Yamazawa, H.: Bulk transfer coefficient over a snow surface, Boundary-Layer Meteorol, 34, 123–135, https://doi.org/10.1007/BF00120912, 1986.

LaChapelle, E.: Secrets of the Snow - Visual Clues to Avalanche and Ski Conditions, University of Washington Press, 2001.

Wallace, J. M. and Hobbs, P. V.: Atmospheric Science: An Introductory Survey, Elsevier, 507 pp., 2006.